Hindawi Publishing Corporation
International Journal of Antennas and Propagation
Volume 2011, Article ID 421691, 7 pages
doi:10.1155/2011/421691

Research Article

An Envelope Correlation Formula for (N, N) MIMO Antenna Arrays Using Input Scattering Parameters, and Including Power Losses

Y. A. S. Dama,[1] R. A. Abd-Alhameed,[1] S. M. R. Jones,[1] D. Zhou,[1] N. J. McEwan,[1] M. B. Child,[1] and P. S. Excell[2]

[1] *Shool of Engineering, Design and Technology, University of Bradford, West Yorkshire, BD7 1DP, UK*
[2] *Centre for Applied Internet Research, Glyndŵr University, Wrexham LL11 2AW, Wales, UK*

Correspondence should be addressed to Y. A. S. Dama, yasdama@bradford.ac.uk

Received 1 June 2011; Revised 3 August 2011; Accepted 5 August 2011

Academic Editor: Hon Tat Hui

The scattering parameter formulation for the envelope correlation in an (N, N) MIMO antenna array has been modified to take the intrinsic antenna power losses into account. This method of calculation provides a major simplification over the use of antenna radiation field patterns. Its accuracy is illustrated in three examples, which also show that the locations of the correlation minima are sensitive to the intrinsic losses.

1. Introduction

MIMO systems employ multiple antennas at transmitter and receiver to improve the reliability and capacity of wireless links in a rich electromagnetic scattering environment. It is well known that the capacity of an (N, N) MIMO system increases with N, the number of antennas in the transmit and receive arrays on the assumption of independent Rayleigh fading between each pair of transmit and receive antennas [1]. In practice, the independence of the received signals will depend on the angular distribution in the channel, the arrangement and radiation pattern of the antennas, and their polarization. It will be reduced by mutual coupling between antennas [2]. The avoidance of mutual coupling and the ability to distinguish between paths arriving at closely spaced angles is favored by larger antenna spacing, whilst practical constraints often demand compact arrangements, especially in mobile systems. To optimize the diversity performance of the array, antennas should be located so as to sample the channel at separations that exhibit minimum spatial correlation [3, 4], taking account of mutual coupling effects [5–7]. (Note that in some circumstances, mutual coupling can enhance MIMO capacity [8, 9].) Since the optimum separation distance will depend on the angle-of-arrival distributions, practical systems may elect to optimize the separation for an average channel, for which a common assumption is of a rich scattering environment with scatterers uniformly distributed in angle. For this reason, it is useful in developing practical systems to have a straightforward means to evaluate the spatial, complex-envelope correlation for the system of antennas [6, 10].

The theory presenting a generalized analysis of signal correlation between any two array elements to include nonidentical elements and arbitrary load termination of passive antenna ports was presented in [11], the method is related to the power balance concept and based on the antenna impedance matrix. In [4, 12], theoretical and simulation studies have been conducted to explain the experimentally observed effect that the correlation between signals of closely spaced antennas is smaller than that predicted using the well-known theoretical methods. A simple expression to compute the correlation coefficients from the far field pattern including the propagation environment characteristic and the terminating impedance was introduced in [13].

There are three possible methods to compute the envelope correlation. The first method is based on the use of far field pattern data [8], and the use of actual or simulated radiation field data is time consuming if spread over several design iterations. The second method employs the scattering parameters measured at the antenna terminals [14], and

there is a third method based on Clarke's formula [15]. The calculation may also be formulated in terms of a generalised impedance matrix [11]. In practice, we require the correlation between any two antennas in an array. In [16] a useful relation was presented including the effect of the antenna efficiencies on the calculated spatial correlation. The correlation is sensitive to the intrinsic power losses in the radiating structures. The scattering formulation derived and tested in [14, 17] does not include these losses, and this provides the rationale for the method presented below.

2. Background Theory

The envelope correlation for two antennas may be calculated from (1):

$$\rho_e = \frac{\left| \iint_{4\pi} d\Omega F_1(\theta,\phi)^* \cdot F_2(\theta,\phi) \right|^2}{\iint_{4\pi} d\Omega \left| F_1(\theta,\phi) \right|^2 \iint_{4\pi} d\Omega \left| F_2(\theta,\phi) \right|^2}, \quad (1)$$

where $F_i(\theta,\phi) = F_\theta^i(\theta,\phi)\hat{a}_\theta + F_\phi^i(\theta,\phi)\hat{a}_\phi$ is the radiation field of the ith antenna and the surface integrations are over the 2-sphere [15]. On this basis, the envelope correlation between antennas i and j may be obtained from (2), as described in [16],

$$\rho_e(i,j,N) = \frac{\left| C_{i,j}(N) \right|^2}{\prod_{k=(i,j)} \left[1 - C_{k,k}(N)\right]}, \quad (2)$$

where $C_{i,j}(N)$ is expressed as

$$C_{i,j}(N) = \sum_{n=1}^{N} S_{i,n}^* S_{n,j}. \quad (3)$$

Hence, from (2) and (3), the explicit scattering parameter formula for envelope correlation is [17]:

$$\rho_e(i,j,N) = \frac{\left| \sum_{n=1}^{N} S_{i,n}^* S_{n,j} \right|^2}{\prod_{k=(i,j)} \left[1 - \sum_{n=1}^{N} S_{i,n}^* S_{n,k}\right]}. \quad (4)$$

Although (4) offers a simple approach compared with radiation pattern, it should be emphasized that this equation is limited by certain three assumptions as in [18].

In this paper, the computed two-antenna envelope correlation for an (N, N) MIMO system will be evaluated from the scattering parameters and the intrinsic power losses in the radiating structures. This calculation represents a significant simplification over using the far field patterns in (1).

3. Summary of the Method

Considering the electromagnetic geometry in Figure 1, the total power is given by

$$P_{\text{total}} = P_{\text{rad}} + P_{\text{loss}}, \quad (5)$$

where P_{rad} and P_{loss} are the total radiated power and power loss, respectively. P_{total} is also known as the accepted power and may be computed in terms of the incident wave, amplitude a and reflected amplitude b by $(a^\dagger a - b^\dagger b)$, where $\dagger$ denotes the Hermitian conjugate.

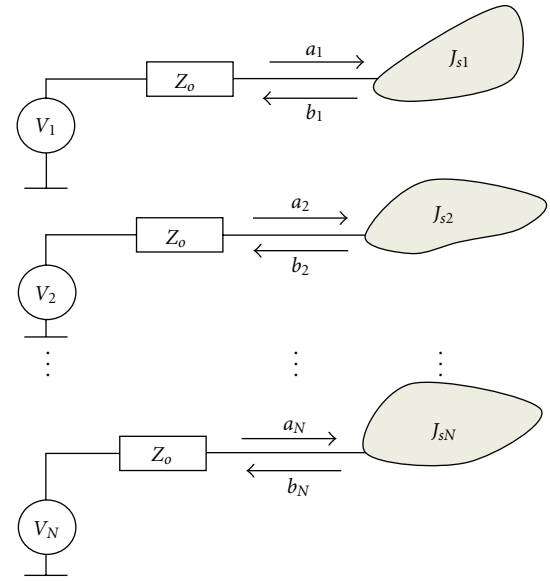

Figure 1: The electromagnetic geometry for the N antenna element system.

The analysis developed below, and the subsequent case studies shown in Figure 2, have been presented for convenience in a wire antenna formulation and the solved using NEC. It should be understood that the underlying concepts are fully general, and can be readily rewritten in terms of general surface and volume currents.

The surface current density on a wire antenna (dipole) structure can be written as

$$J_s(\theta,l) = \frac{I(\theta,l)}{2\pi r}\hat{a}_l \approx \frac{I(l)}{2\pi r}\hat{a}_l, \quad (6)$$

where r is the radius of the dipole wire.

The power loss may be computed in terms of the surface currents on the antenna structures as follows. These currents may be expressed in terms of the incident waves $a_1, a_2, \ldots a_n$

$$\begin{aligned}
J_{s1} &= \frac{1}{\sqrt{R_s}}\left(a_1 \cdot \frac{I_{11}(l)}{2\pi r}\hat{a}_l + a_2 \cdot \frac{I_{12}(l)}{2\pi r}\hat{a}_l + a_3 \cdot \frac{I_{13}(l)}{2\pi r}\hat{a}_l \right.\\
&\qquad \left. + \cdots + a_N \cdot \frac{I_{1N}(l)}{2\pi r}\hat{a}_l\right),\\
J_{s2} &= \frac{1}{\sqrt{R_s}}\left(a_1 \cdot \frac{I_{21}(l)}{2\pi r}\hat{a}_l + a_2 \cdot \frac{I_{22}(l)}{2\pi r}\hat{a}_l + a_3 \cdot \frac{I_{23}(l)}{2\pi r}\hat{a}_l \right.\\
&\qquad \left. + \cdots + a_N \cdot \frac{I_{2N}(l)}{2\pi r}\hat{a}_l\right), \quad (7)\\
&\vdots\\
J_{si} &= \frac{1}{\sqrt{R_s}}\left(a_1 \cdot \frac{I_{i1}(l)}{2\pi r}\hat{a}_l + a_2 \cdot \frac{I_{i2}(l)}{2\pi r}\hat{a}_l + a_3 \cdot \frac{I_{i3}(l)}{2\pi r}\hat{a}_l \right.\\
&\qquad \left. + \cdots + a_N \cdot \frac{I_{iN}(l)}{2\pi r}\hat{a}_l\right).
\end{aligned}$$

The I_{iN} terms are the normalised currents on structure i due to the incident wave N, and R_s is the surface impedance of

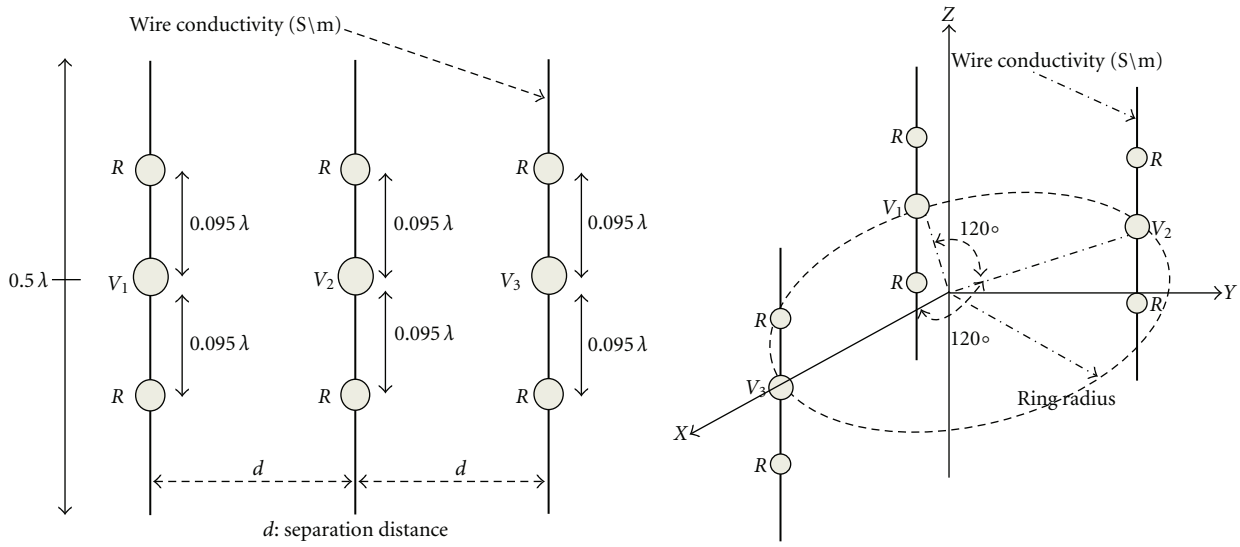

Figure 2: Examples under test: (a) Uniform linear array, (b) Ring array.

the antenna. The power loss on the ith antenna structure is calculated by

$$P_{\text{loss}_i} = \iint J_{si} \cdot J_{s_i}^{*} r d\theta dl,$$

$$\begin{aligned} P_{\text{loss}_i} = \iint \Bigg\{ & a_1 \cdot a_1^{*} \frac{I_{i1}(l) I_{i1}^{*}(l)}{(2\pi r)^2} + a_1 \cdot a_2^{*} \frac{I_{i1}(l) I_{i2}^{*}(l)}{(2\pi r)^2} \\ & + \cdots + a_1 \cdot a_N^{*} \frac{I_{i1}(l) I_{iN}^{*}(l)}{(2\pi r)^2} + a_2 \cdot a_1^{*} \frac{I_{i2}(l) I_{i1}^{*}(l)}{(2\pi r)^2} \\ & + a_2 \cdot a_2^{*} \frac{I_{i2}(l) I_{i2}^{*}(l)}{(2\pi r)^2} + \cdots + a_2 \cdot a_N^{*} \frac{I_{i2}(l) I_{iN}^{*}(l)}{(2\pi r)^2} \\ & + \cdots + a_N \cdot a_1^{*} \frac{I_{iN}(l) I_{i1}^{*}(l)}{(2\pi r)^2} + a_N \cdot a_2^{*} \frac{I_{iN}(l) I_{i2}^{*}(l)}{(2\pi r)^2} \\ & + \cdots + a_N \cdot a_N^{*} \frac{I_{iN}(l) I_{iN}^{*}(l)}{(2\pi r)^2} \Bigg\} r d\theta dl, \end{aligned} \tag{8}$$

solving for circumferential integral leads to

$$\begin{aligned} P_{\text{loss}_i} = \frac{1}{2\pi r} \int_l \Big\{ & a_1 \cdot a_1^{*} I_{i1}(l) I_{i1}^{*}(l) + a_1 \cdot a_2^{*} I_{i1}(l) I_{i2}^{*}(l) + \cdots \\ & + a_1 \cdot a_N^{*} I_{i1}(l) I_{iN}^{*}(l) + a_2 \cdot a_1^{*} I_{i2}(l) I_{i1}^{*}(l) dl \\ & + a_2 \cdot a_2^{*} I_{i2}(l) I_{i2}^{*}(l) dl + \cdots \\ & + a_2 \cdot a_N^{*} I_{i2}(l) I_{iN}^{*}(l) + a_N \cdot a_1^{*} I_{iN}(l) I_{i1}^{*}(l) \\ & + \cdots + a_N \cdot a_2^{*} I_{iN}(l) I_{i2}^{*}(l) + \cdots \\ & + a_N \cdot a_N^{*} I_{iN}(l) I_{iN}^{*}(l) \Big\} dl. \end{aligned} \tag{9}$$

Subject to (9), the power losses may be expressed in matrix notation as follows,

$$P_{\text{loss}} = a^{\dagger} L a, \tag{10}$$

where the linear operator L can be defined by the following:

$$L = L^1 + L^2 + L^3 + \cdots + L^i. \tag{11}$$

The matrix representations of the elements of L, as example L^1 and L^i can be written as below:

$$L^1 = \frac{1}{2\pi r} \begin{bmatrix} \int_l I_{11}(l) I_{11}^{*}(l) dl & \int_l I_{11}(l) I_{12}^{*}(l) dl & \cdots & \int_l I_{11}(l) I_{1N}^{*}(l) dl \\ \int_l I_{12}(l) I_{11}^{*}(l) dl & \int_l I_{12}(l) I_{12}^{*}(l) dl & \cdots & \int_l I_{12}(l) I_{1N}^{*}(l) dl \\ \vdots & \vdots & \cdots & \cdots \\ \int_l I_{1N}(l) I_{11}^{*}(l) dl & \int_l I_{1N}(l) I_{12}^{*}(l) dl & \cdots & \int_l I_{1N}(l) I_{1N}^{*}(l) dl \end{bmatrix},$$

$$\vdots$$

$$\vdots$$

$$L^i = \frac{1}{2\pi r} \begin{bmatrix} \int_l I_{i1}(l) I_{i1}^{*}(l) dl & \int_l I_{i1}(l) I_{i2}^{*}(l) dl & \cdots & \int_l I_{i1}(l) I_{iN}^{*}(l) dl \\ \int_l I_{i2}(l) I_{i1}^{*}(l) dl & \int_l I_{i2}(l) I_{i2}^{*}(l) dl & \cdots & \int_l I_{i2}(l) I_{iN}^{*}(l) dl \\ \vdots & \vdots & \cdots & \cdots \\ \int_l I_{iN}(l) I_{i1}^{*}(l) dl & \int_l I_{iN}(l) I_{i2}^{*}(l) dl & \cdots & \int_l I_{iN}(l) I_{iN}^{*}(l) dl \end{bmatrix}. \tag{12}$$

Hence the energy balance for the system expressed through (5) may be re-expressed fully in terms of the incident wave amplitudes, and the scattering matrix $S \in \mathbb{C}^{N\times N}$,

$$a^{\dagger}\left(1 - S^{\dagger}S\right)a = a^{\dagger}La + a^{\dagger}Ra. \tag{13}$$

This is essentially a modification of Stein's formulation for a multi-beam array [19], where R is a general $N \times N$ matrix. The explicit form of R is as follows,

$$R = \begin{pmatrix} \frac{D_1}{4\pi}\iint_{4\pi} d\Omega \left|F_1(\theta,\phi)\right|^2 & \frac{\sqrt{D_1D_2}}{4\pi}\iint_{4\pi} d\Omega F_1(\theta,\phi)\cdot F_2^*(\theta,\phi) & \cdots & \frac{\sqrt{D_1D_N}}{4\pi}\iint_{4\pi} d\Omega F_1(\theta,\phi)\cdot F_N^*(\theta,\phi) \\ \frac{\sqrt{D_2D_1}}{4\pi}\iint_{4\pi} d\Omega F_2(\theta,\phi)\cdot F_1^*(\theta,\phi) & \frac{D_2}{4\pi}\iint_{4\pi} d\Omega \left|F_2(\theta,\phi)\right|^2 & \cdots & \frac{\sqrt{D_2D_N}}{4\pi}\iint_{4\pi} d\Omega F_2(\theta,\phi)\cdot F_N^*(\theta,\phi) \\ \vdots & \vdots & \cdots & \cdots \\ \frac{\sqrt{D_ND_1}}{4\pi}\iint_{4\pi} d\Omega F_N(\theta,\phi)\cdot F_1^*(\theta,\phi) & \frac{\sqrt{D_ND_2}}{4\pi}\iint_{4\pi} d\Omega F_N(\theta,\phi)\cdot F_2^*(\theta,\phi) & \cdots & \frac{D_N}{4\pi}\iint_{4\pi} d\Omega \left|F_N(\theta,\phi)\right|^2 \end{pmatrix}, \tag{14}$$

where D_i is the maximum directivity of the ith antenna.

Now, considering the above equations, the envelope correlation between the antennas i and j in the (N,N) MIMO system can be expressed in terms of the scattering parameters and the intrinsic power losses as follows:

$$\rho_e(i,j,N) = \frac{\left|\sum_{n=1}^{N} S_{i,n}^{*}S_{n,j}^{*} - \sum_{n=1}^{N} L_{ij}^{n}\right|^2}{\prod_{k=i,j}\left[1 - \sum_{n=1}^{N} S_{k,n}^{*}S_{n,k} - \sum_{n=1}^{N} L_{kk}^{n}\right]}. \tag{15}$$

As an example, for a (3,3) MIMO system (i.e., three-antennas at each end), the spatial correlation between antennas 1 and 2 may be calculated directly from the following,

$$\rho_e(1,2,3) = \frac{\left|S_{11}^{*}S_{12} + S_{12}^{*}S_{22} + S_{13}^{*}S_{32} - \left(L_{12}^{1} + L_{12}^{2} + L_{12}^{3}\right)\right|}{\left[1 - \left(|S_{11}|^2 + |S_{21}|^2 + |S_{31}|^2\right) - \left(L_{11}^{1} + L_{11}^{2} + L_{11}^{3}\right)\right]\left[1 - \left(|S_{22}|^2 + |S_{12}|^2 + |S_{32}|^2\right) - \left(L_{22}^{1} + L_{22}^{2} + L_{22}^{3}\right)\right]}. \tag{16}$$

4. Simulation and Results

To verify (16), the spatial envelope correlation has been computed between two half wavelength dipole antennas, in free space for a three-antenna system, as a function of their separation distance. The far field and scattering parameters have been computed using the NEC code.

For this example, the dipole radius for each structure was set to 0.002 wavelengths. Three different sources of loss were considered for validation purposes, and two distinct MIMO configurations were investigated, namely, a uniform linear array, and a circular (ring) array. In each case, the three dipoles were loaded by two lumped 25 Ω resistive loads, separated by 0.095 wavelengths from the input source, as shown in Figure 2. The excitation was simply modeled by a voltage source at the centre of each dipole, and the applied termination load is 50 Ω.

Departures between the results of this method and the lossless approach were checked through simulation. The spatial envelope correlations between the antenna elements 1 and 2 in the three element uniform linear array were calculated using the far field as a function of the dipole separation distances. The results are presented in Figure 3 for the lossy and lossless cases. Close agreement may be observed between the lossy analysis derived from (16), and the far field analysis in (1). The envelope correlation for dipole separation distances less than 0.5 wavelengths and between each of the intervals from 0.8 to 0.9 wavelengths, 1.35 to 1.45 wavelengths and 1.85 to 1.95 wavelengths can take values bigger than the achieved S_{21} values. It is also interesting to note that the nulls of the spatial envelope correlation are shifted as compared with those computed via the lossless approach.

In Figure 4, the spatial envelope correlation between dipole elements 1 and 3 in the same uniform linear array are recorded, also as a function of their separation distance, for both lossy and lossless cases. It can be seen that the correlation values for the lossless case are smaller than for the lossy case, this is due to the middle element acting as a perfect reflector in the lossless case, thus contributing to a higher reflected power as compared to radiation power. The separation distance between the two radiators will affect the transmittance, $|S_{21}|$ which is associated with their mutual coupling.

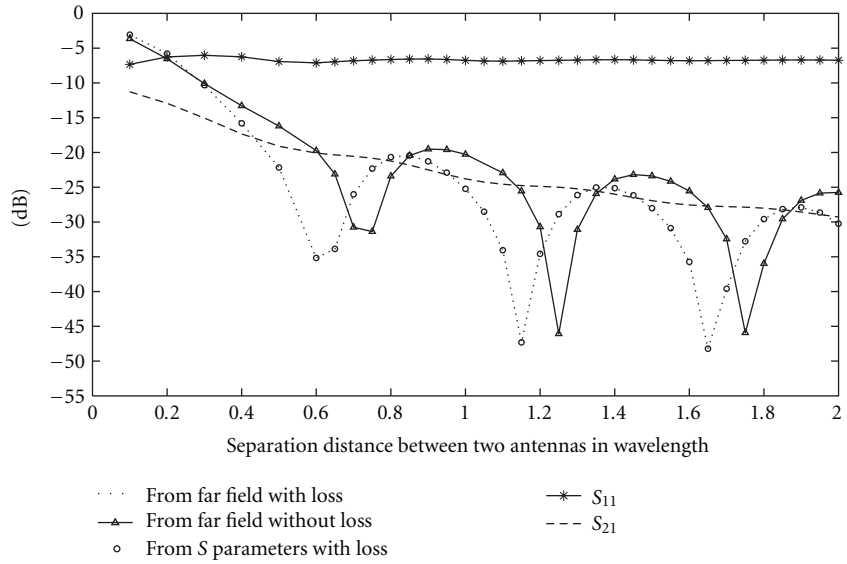

Figure 3: The computed spatial envelope correlations and scattering parameters between dipoles 1 and 2 versus their separation distance, in a MIMO system of three elements, arranged in a uniform linear array.

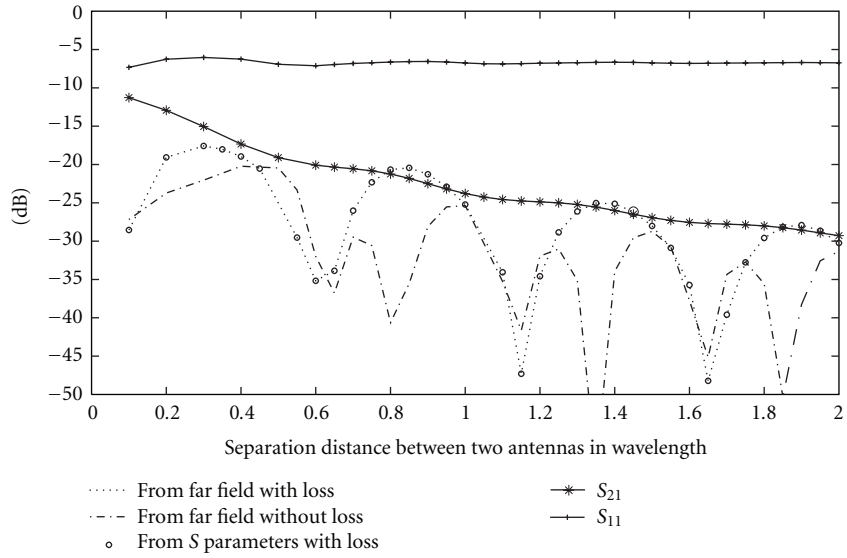

Figure 4: The computed spatial envelope correlations and scattering parameters between dipoles 1 and 3 versus their separation distance, in a MIMO system of three elements, arranged in a uniform linear array.

In Figure 5, the spatial envelope correlation between dipole elements 1 and 2 in a three-antenna element ring array are recorded as a function of the ring radius in wavelengths, for both the lossy and lossless cases. These results show close agreement between the lossy analysis and the far field analysis from (1). For dipole separation less than 0.15 wavelengths and in the interval between 0.4 to 0.55 wavelengths the spatial envelope correlation can take values bigger than the S_{21} values. Furthermore, the nulls of the envelope correlation calculated by the current method are shifted compared with the corresponding values from the lossless calculation, indicating the significance of including the intrinsic losses in the calculations. The spatial envelope correlations between elements 2 and 3, and 1 and 3, in the ring array will be the same as for 1 and 2 due to symmetry.

Figure 6 depicts the variation of the spatial envelope correlation between dipole elements 1 and 2 versus the surface conductivities for a three-antenna element uniform linear array and a ring array. The separation distance between the parallel dipoles in the case of the uniform linear array was kept constant at 0.5 wavelengths, and in the case of the ring array the ring radius was set to 0.5 wavelengths. It can be noted, from Figure 6 that the envelope correlation values become unaffected when the values of the surface conductivities get higher. Also, it is noticeable from Figure 6 that the envelope correlation values are within 1 dB and

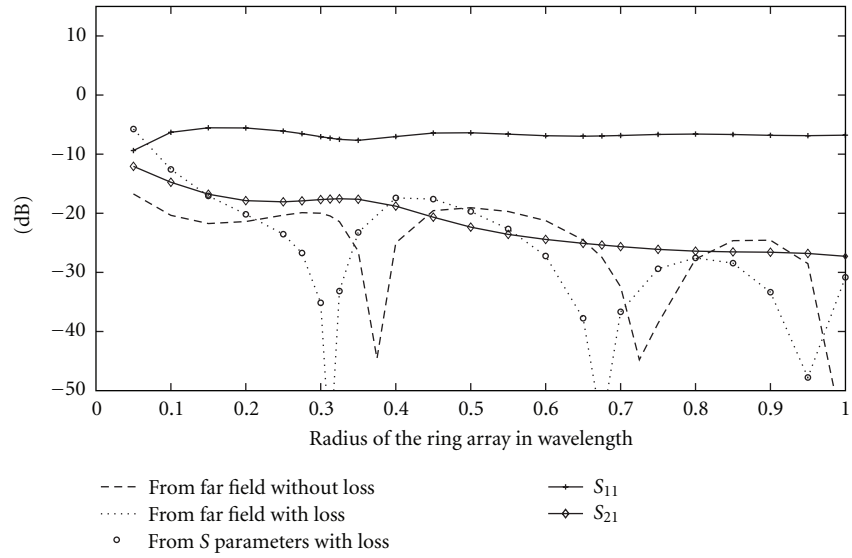

Figure 5: The computed spatial envelope correlations and scattering parameters between dipoles 1 and 2 versus their separation distance, in a MIMO system of three elements, arranged in a ring array.

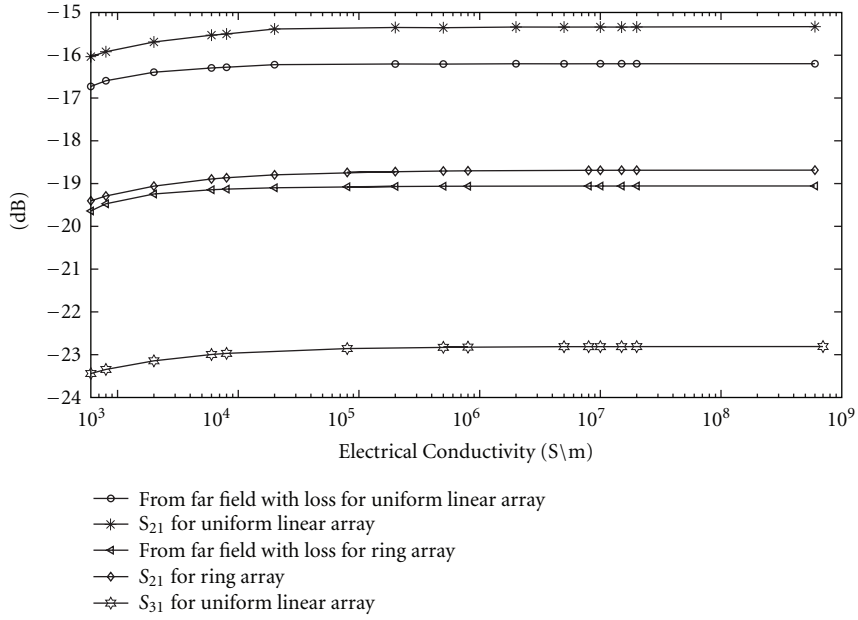

Figure 6: The computed spatial envelope correlations and scattering parameters between dipoles 1 and 2 versus their wire electric conductivity, in a MIMO system of three elements, arranged in a uniform linear array and in a ring array.

0.5 dB of the S_{21} values for the uniform linear array and ring array, respectively.

In summary, the analysis described here, based on the conceptual framework summarized in (16), provides a direct and accurate forecast of spatial envelope correlations, as compared with those obtained from the far field data in (1).

5. Conclusion

A direct calculation method has been presented for the spatial envelope correlation between any two antennas in a (N, N) MIMO array using the scattering parameters and intrinsic losses in the radiating structures. This formula should reduce the complexity and effort involved in spatial envelope correlation calculations for practical designs especially where low envelope correlation is required. Three examples have been presented to validate the technique. The results have shown close agreement between this method and the full computation using the far field pattern data. Several practical methods exist, for example, radiometer [20, 21], random field [22], and reverberation chamber [23], for direct measurement of the radiation efficiency of passive

antennas. These can be used for multiport structures and can provide independent checks of the diagonal terms in (12). Such practical implementations of the proposed method will be considered further in future work.

Acknowledgment

The authors would like to thank Pace PLC (Saltaire, West Yorkshire, BD18 3LF) for their financial support of the Knowledge Transfer Partnership (KTP no. 7277).

References

[1] G. J. Foschini and M. J. Gans, "On limits of wireless communications in a fading environment when using multiple antennas," *Wireless Personal Communications*, vol. 6, pp. 311–335, 1998.

[2] R. Janaswamy, "Effect of element mutual coupling on the capacity of fixed length linear arrays," *IEEE Antennas and Wireless Propagation Letters*, vol. 1, pp. 157–160, 2002.

[3] R. G. Vaughan and J. B. Andersen, "Antenna diversity in mobile communications," *IEEE Transactions on Vehicular Technology*, vol. 36, no. 4, pp. 149–172, 1987.

[4] R. G. Vaughan and N. L. Scott, "Closely spaced monopoles for mobile communications," *Radio Science*, vol. 28, no. 6, pp. 1259–1266, 1993.

[5] M. K. Ozdemir, H. Arslan, and E. Arvas, "On the correlation analysis of antennas in adaptive MIMO systems with 3-D multipath scattering," in *Proceedings of the IEEE Wireless Communications and Networking Conference (WCNC '04)*, vol. 1, pp. 295–299, 2004.

[6] T. S. P. See, A. M. L. Swee, and Z. N. Chen, "Correlation analysis of UWB MIMO antenna system configurations," in *Proceedings of the IEEE International Conference on Ultra-Wideband (ICUWB '08)*, pp. 105–108, Hannover, Germany, September 2008.

[7] A. A. H. Azremi, M. Kyro, J. Ilvonen et al., "Five-element in-verted-F antenna array for MIMO communications and radio direction finding on mobile terminal," in *Proceedings of the Loughborough Antennas and Propagation Conference (LAPC '09)*, pp. 557–560, November 2009.

[8] S. S. G. Lebrun and M. Faulkner, "MIMO complexity reduction through antenna selection," *Proceedings of the Australian Telecommunications Cooperative Research Centre*, vol. 5, pp. 1–5, 2003.

[9] H. Zhang, Z. Wang, J. Yu, and J. Huang, "A compact MIMO antenna for wireless communication," *IEEE Antennas and Propagation Magazine*, vol. 50, no. 6, pp. 104–107, 2008.

[10] T. S. P. See and Z. N. Chen, "An ultrawideband diversity antenna," *IEEE Transactions on Antennas and Propagation*, vol. 57, no. 6, pp. 1597–1605, 2009.

[11] A. Derneryd and G. Kristensson, "Signal correlation including antenna coupling," *Electronics Letters*, vol. 40, no. 3, pp. 157–159, 2004.

[12] P. S. H. Leather and D. Parsons, "Antenna diversity for UHF handportable radio," *Electronics Letters*, vol. 39, no. 13, pp. 946–948, 2003.

[13] A. Derneryd and G. Kristensson, "Antenna signal correlation and its relation to the impedance matrix," *Electronics Letters*, vol. 40, no. 7, pp. 401–402, 2004.

[14] S. Blanch, J. Romeu, and I. Corbella, "Exact representation of antenna system diversity performance from input parameter description," *Electronics Letters*, vol. 39, no. 9, pp. 705–707, 2003.

[15] R. H. Clarke, "A statistical theory of mobile reception," *Bell Systems Technical Journal*, vol. 47, pp. 957–1000, 1968.

[16] P. Hallbjörner, "The significance of radiation efficiencies when using S-parameters to calculate the received signal correlation from two antennas," *IEEE Antennas and Wireless Propagation Letters*, vol. 4, no. 1, pp. 97–99, 2005.

[17] J. Thaysen and K. B. Jakobsen, "Envelope correlation in (N,N) mimo antenna array from scattering parameters," *Microwave and Optical Technology Letters*, vol. 48, no. 5, pp. 832–834, 2006.

[18] A. Diallo, P. Le Thuc, C. Luxey et al., "Diversity characterization of optimized two-antenna systems for UMTS handsets," *Eurasip Journal on Wireless Communications and Networking*, vol. 2007, Article ID 37574, 9 pages, 2007.

[19] S. Stein, "On cross coupling in multiple-beam antennas," *IRE Transactions on Antennas and Propagation*, vol. 10, pp. 548–557, 1962.

[20] N. J. McEwan, R. A. Abd-Alhameed, and M. N. Z. Abidin, "A modified radiometric method for measuring antenna radiation efficiency," *IEEE Transactions on Antennas and Propagation*, vol. 51, no. 8, pp. 2099–2105, 2003.

[21] W. L. Schroeder and D. Gapski, "Direct measurement of small antenna radiation efficiency by calorimetric method," *IEEE Transactions on Antennas and Propagation*, vol. 54, no. 9, pp. 2646–2656, 2006.

[22] Q. Chen, H. Yoshioka, K. Igari, and K. Sawaya, "Comparison of experimental methods for measuring radiation efficiency of antennas for portable telephone," in *Proceedings of the IEEE Antennas and Propagation Society International Symposium*, vol. 1, pp. 149–152, June 1998.

[23] K. Rosengren and P.-S. Kildal, "Radiation efficiency, correlation, diversity gain and capacity of a six-monopole antenna array for a MIMO system: theory, simulation and measurement in reverberation chamber," *IEE Proceedings of Microwaves, Antennas and Propagation*, vol. 152, no. 1, pp. 7–16, 2005.